ACTIVE CONTROL OF COUPLED AXIAL AND TORSIONAL DRILL-STRING VIBRATIONS

Marcelo A. Trindade
Department of Mechanical Engineering, São Carlos School of Engineering, University of São Paulo, Av. Trabalhador São-Carlense, 400, São Carlos-SP, 13566-590, Brazil
trindade@sc.usp.br

Rubens Sampaio
Department of Mechanical Engineering, Pontifícia Universidade Católica do Rio de Janeiro, rua Marquês de São Vicente, 225, Rio de Janeiro-RJ, 22453-900, Brazil
rsampaio@mec.puc-rio.br

Abstract. *Drilling operations for oil and gas wells requires the control of a very flexible structure subjected to complex boundary conditions. One of the most important causes of failure in drill-strings and drill-bits is the stick-slip phenomenon occurring at drill-bit/formation interface. Although several works on drill-string dynamics have been recently published in the literature, the effect of axial excitation on stick-slip phenomenon and, more importantly, on drilling performance is still an open question. Hence, the coupling between axial and torsional vibrations and its effects on the drilling performance are studied in the present work, using an axial-torsional finite element model. The drill-bit-formation interaction is modelled using a nonlinear regularized friction model which accounts for the dynamical behavior of the reaction force at bit-formation interface. Numerical results confirm that a standard PI control driving system leads to a fluctuating drill-bit angular velocity. Then, an alternative drilling condition using axial excitations at the top-drive, combined to an axial direct velocity feedback controller, to minimize rate-of-penetration oscillations is tested, showing satisfactory results.*

Keywords: *Drill-string dynamics, active vibration control, stick-slip, driving rotary speed control*

1. Introduction

Drilling operations for oil and gas wells involves rock crushing by a rotating drill-bit whose rotation is driven by a torque drive system at the surface (top position), through a drill-string that transmits torque to the drill-bit (bottom position). Specially for deep wells, this operation requires the control of a very flexible structure (the drill-string length may be up to 5 km whereas its diameter is typically less than 15 cm) subjected to complex boundary conditions, due mainly to the interactions between drill-bit and rock formation. One of the most important causes of malfunctioning or failure of drill-strings and drill-bits is the stick-slip phenomenon occurring between the drill-bit and rock formation (Jansen and van den Steen, 1995). Due to this phenomenon, a standard control driving system designed to maintain a nearly constant angular velocity at the top-drive may lead to a fluctuating drill-bit angular velocity. In extreme cases, these oscillations may lead to complete standstill of the drill-bit (stick phase), during which the drill-string is torqued-up, until the drill-bit rotation is released (slip phase) and rotates at an angular velocity much higher than the target one. This phenomenon has been identified as a periodic and stable oscillation of drilling rotational speed during several field observations (Plácido, Santos and Galeano, 2004). Stick-slip oscillations are self-excited and generally disappear as the target angular velocity is increased. However, higher angular velocities may lead to lateral vibration (backward and forward whirling), impacts of drill-string and borehole wall, and parametric instabilities. Lateral (bending) vibrations may also lead to complex vibrational states since it is normally coupled to the axial vibrations (Trindade, Wolter and Sampaio, 2005; Trindade and Sampaio, 2002). Hence, it is desirable to improve drilling conditions at relatively low angular velocities. Several works on drill-string dynamics have been recently published in the literature focusing on dynamical models and control strategies. Yigit and Christoforou (2000, 2003) have presented a discrete model for a drill-string cross-section, while Tucker and Wang (2003) used a special Cosserat theory of rods to model the drill-string as a continuum. In both works (Christoforou and Yigit, 2003; Tucker and Wang, 2003), a frictional torque model in terms of drill-bit angular velocity and weight-on-bit is considered. However, it is still not very clear how a dynamic weight-on-bit, induced by an axial excitation, may affect the stick-slip phenomenon and, more importantly, the drilling performance. Hence, the coupling between axial and torsional vibrations and its effects on the drilling performance are studied in the present work, using an axial-torsional finite element model.

2. Drill-string Dynamics Modelling

Let us consider an initially straight and slender drill-string, of undeformed length L and outer and inner radii R_o and R_i, undergoing small axial and torsional displacements and deformations as shown in Figure 1.

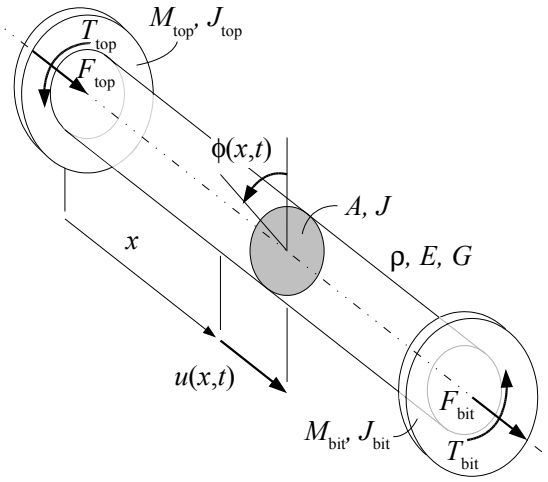

Figure 1. Drill-string undergoing axial and torsional displacements and deformations.

2.1 Equations of Motion and Boundary Conditions

Small deformations are assumed so that the drill-string behaves as linear elastic. Hence, the following equations for axial and torsional vibrations of bars are used

$$\rho A\ddot{u}(x,t) - EAu''(x,t) = \rho Ag \;\text{ and }\; \rho J\ddot{\phi}(x,t) - GJ\phi''(x,t) = 0 \tag{1}$$

where the x direction is considered to be the vertical one and, hence, the right hand side term ρAg in the first equation stands for the distributed weight.

The drill-string is assumed to be connected to rigid bodies with effective masses $M_{\rm top}$ and $M_{\rm bit}$, and rotary inertias $J_{\rm top}$ and $J_{\rm bit}$, corresponding to simplified models for the top-drive and drill-bit, respectively. The top-drive is connected to the drill-string at $x = 0$ and the drill-bit is located at $x = L$. Point forces, $F_{\rm top}$ and $F_{\rm bit}$, and torques, $T_{\rm top}$ and $T_{\rm bit}$, are considered at the top-drive and drill-bit, respectively. Consequently, four boundary conditions may be written for the drill-string axial and torsional vibrations in the form

$$\begin{aligned} M_{\rm top}\ddot{u}(0,t) - EAu'(0,t) = F_{\rm top}(t), \quad M_{\rm bit}\ddot{u}(L,t) + EAu'(L,t) = F_{\rm bit}(t), \\ J_{\rm top}\ddot{\phi}(0,t) - GJ\phi'(0,t) = T_{\rm top}(t), \quad J_{\rm bit}\ddot{\phi}(L,t) + GJ\phi'(L,t) = T_{\rm bit}(t). \end{aligned} \tag{2}$$

2.2 Finite Element Model

The finite element model is constructed using a Lagrange linear discretization of axial and torsional displacements, $u(x,t)$ and $\phi(x,t)$. This leads to a finite element with four degrees of freedom $\{u_1\ \phi_1\ u_2\ \phi_2\}$. Using these expressions and assembling elements, yields discretized equations of motion

$$\mathbf{M}\ddot{\mathbf{q}} + \mathbf{D}\dot{\mathbf{q}} + \mathbf{K}\mathbf{q} = \mathbf{F}_x + \mathbf{T}_c + \mathbf{T}_r \tag{3}$$

where $\ddot{\mathbf{q}}$ is the acceleration vector and $\mathbf{D}$ a damping matrix added a posteriori. The vector $\mathbf{F}_x$ is the distribution, through the finite element degrees of freedom, of all axial forces, including the distributed gravity forces ρAg, the top-hook load $F_{\rm top}(t)$ and the bit reaction force (due to the dynamic weight-on-bit) $F_{\rm bit}(t)$. The applied torque at the top-drive $T_{\rm top}(t)$ is accounted for as a control torque vector $\mathbf{T}_c$ and the bit-reaction torque $T_{\rm bit}(t)$, due to cutting and frictional torques, is represented in the reaction torque vector $\mathbf{T}_r$.

2.3 Initial Static Hanging Configuration

The initial static hanging configuration is evaluated by first considering that the drill-string is fixed at the top $u(0,t) = 0$ and free at the drill-bit. Then, a initial negative static reaction force $F_{\rm bit}$ is applied to the drill-bit leading to a realistic

configuration for which the upper part of the drill-string is under extension and the lower part of the drill-string is under compression. In the practical case, the drill-string is lowered until the drill-bit touches the formation. In the event of continued lowering, the reaction force of the formation $F_{\rm bit}$, applied to the drill-bit, grows and the lower part of the drill-string is compressed. In the present work, it is supposed that after this quasi-static lowering and when the reaction force reaches a given value, the axial displacement of the drill-bit is locked (Figure 2c). Therefore, further motions occur around this initial deformed configuration, which is the solution of $\mathbf{K}\mathbf{q}_s = \mathbf{F}_x$. This holds because both $\mathbf{T}_c$ and $\mathbf{T}_r$ are initially zero, that is, there is neither driving control torque nor friction. Since the drill-string is supposed to be initially straight and only axial components of both gravity, top-drive and reaction forces are non null, one may expect that only axial displacements will not vanish in $\mathbf{q}_s$.

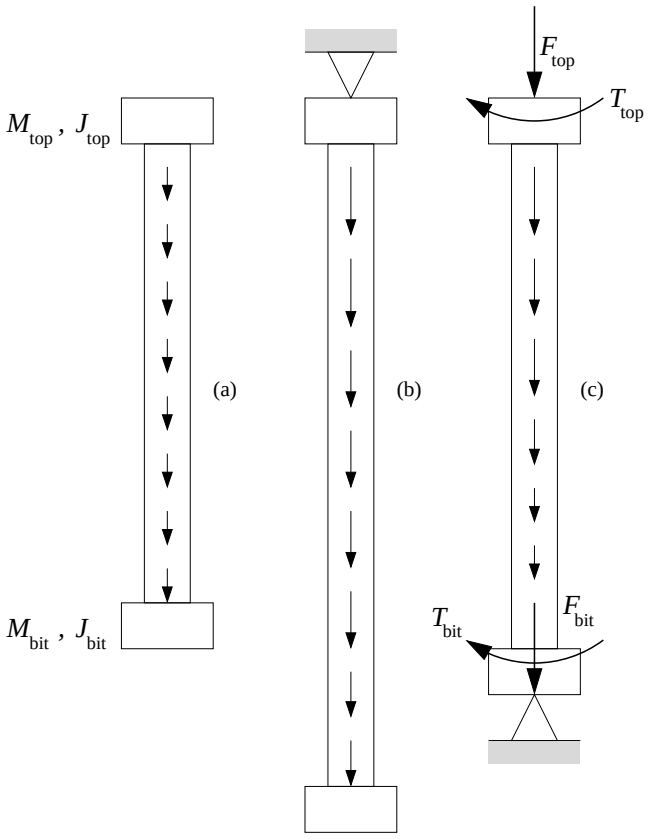

Figure 2. Drill-string configurations: (a) undeformed, (b) static deformation due to weight, and (c) static deformation due to weight and bit reaction.

2.4 Cutting and Friction Modelling

The reaction torque at the drill-bit $T_{\rm bit}(t)$ is assumed to be due only to the interaction between the drill-bit and the rock surface. Consequently, a model for this interaction must be included. It is well-known that stick-slip phenomenon may occur between the drill-bit and the rock surface for certain drilling operation conditions, specially for low angular velocity and large weight-on-bit. Although the reaction torque is also dependent on rock properties, bit geometry and others, it is written here in terms of the drill-bit angular velocity and dynamic weight-on-bit using a model presented by Tucker and Wang (2003). The model was obtained from recent drilling measurements under stable drilling conditions and correlates the frictional torque-on-bit (TOB), drill-bit angular velocity (Ω), weight-on-bit (WOB), depth-of-cut (DOC), and rate-of-penetration (ROP) as

$$\text{TOB} = a_4\text{DOC} + a_5\ ,\ \text{DOC} = \text{ROP}/\Omega\ ,\ \text{ROP} = -a_1 + a_2\text{WOB} + a_3\Omega\ , \tag{4}$$

where $a_1 = 3.429\ 10^{-3}$ m s^{-1}, $a_2 = 5.672\ 10^{-8}$ m N^{-1} s^{-1}, $a_3 = 1.374\ 10^{-4}$ m rad^{-1}, $a_4 = 9.537\ 10^{6}$ N rad, $a_5 = 1.475\ 10^{3}$ N m, for $\Omega \approx 100$ RPM and WOB ≈ 100 kN.

These relations can also be combined to express the friction torque-on-bit directly in terms of the weight-on-bit and drill-bit angular velocity

$$\text{TOB} = \frac{(-a_1 + a_2\text{WOB})a_4}{\Omega} + a_3 a_4 + a_5 \tag{5}$$

In order to model Coulomb frictional effects however, it is necessary to regularize the frictional torque and rate-of-penetration so that they vanish as the drill-bit angular velocity approaches zero from both positive and negative values. This can be achieved by writing

$$T_{\text{bit}} = (-a_1 + a_2 F_{\text{bit}})a_4 \frac{\dot{\phi}_L^3}{(\dot{\phi}_L^2 + \epsilon^2)^2} + a_3 a_4 \frac{\dot{\phi}_L^3}{(\dot{\phi}_L^2 + \epsilon^2)^{(3/2)}} + a_5 \frac{\dot{\phi}_L}{(\dot{\phi}_L^2 + \epsilon^2)^{(1/2)}} \tag{6}$$

where the variables TOB, Ω and WOB were replaced by T_{bit}, $\dot{\phi}_L = \dot{\phi}(L,t)$ and F_{bit}. The behavior of the frictional torque T_{bit} at the drill-bit as a function of its angular velocity $\dot{\phi}_L$ is shown in Figure 3 for three different and constant values of weight-on-bit, where a value of 2 rad/s is chosen for ϵ to simulate the Coulomb friction characteristics at low angular velocity. Notice however that the weight-on-bit F_{bit} can be also time-variant, so that the frictional profile shown in Figure 3 will present a dynamic profile.

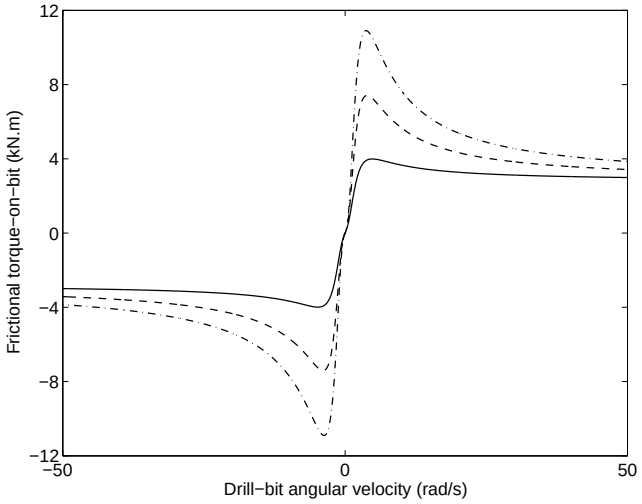

Figure 3. Frictional torque-on-bit in terms of the drill-bit angular velocities for some values of weight-on-bit. —: F_{bit} = 80 kN, – –: F_{bit} = 120 kN, –.: F_{bit} = 160 kN.

3. Rotary Speed Control

The boundary conditions at the top-drive are normally determined by applied hook-load force F_{top} and driving torque T_{top}. The hook-load force F_{top} is meant to support the weight of the drill-string and its attachments. During a typical drilling process, its magnitude is reduced by a factor of a few percent in order to induce a constant target weight-on-bit.

The driving control torque T_{top} has the function of driving the rotary motion of the drill-string. In general, some feedback control strategy is used to evaluate the driving control torque so as to maintain a constant target angular velocity of the drill-string. Here, a standard PI (proportional-integral) rotary speed controller is considered to maintain an angular velocity Ω_r at the top-drive through the application of the following torque

$$T_{\text{top}} = k_p(\Omega_r - \dot{\phi}_0) + k_i(\Omega_r t - \phi_0) \tag{7}$$

Notice, however, that the controller feeds back the difference between the reference angular motion, Ω_r and $\Omega_r t$, and top-drive angular motion, $\dot{\phi}_0 = \dot{\phi}(0,t)$ and $\phi_0 = \phi(0,t)$, that is at $x = 0$. This is often the case since angular displacements and velocities of the drill-string are only measurable at the top-drive. However, due to drill-string torsional vibration and frictional torque at the drill-bit, this does not guarantee a constant target angular velocity Ω_r at the drill-bit. On the other hand, although this simple control strategy will normally yield a fluctuating drill-bit angular velocity, it does not destabilize the system since the angular displacement and velocity sensors and torque actuator are collocated.

In practical drilling conditions, where both torsional vibrations and frictional torque at the drill-bit are present, the choice of proportional and integral gain parameters, k_p and k_i, is quite complex. On one hand, torsional vibrations include a very flexible element between driving torque and target drill-bit angular velocity, leading to both an actuation delay and torsional waves reflection to the top-drive. On the other hand, the frictional torque at the drill-bit presents a highly non-linear behavior, typical of Coulomb friction, as represented by the specific present model (Figure 3), transforming the linear elastic system into a non-linear system for which the linear controller cannot guarantee asymptotic stability.

Table 1. Numerical values for typical drilling parameters.

ρ	Drill-string mass density	8 010 kg m^{-3}
E	Drill-string Young's modulus	207.0 GPa
G	Drill-string shear modulus	79.6 GPa
L	Drill-string length	3 000 m
R_o	Drill-string outer radius	0.0635 m
R_i	Drill-string inner radius	0.0543 m
g	Gravity acceleration	9.81 m s^{-2}
M_{top}	Top-drive effective mass	50 800 kg
J_{top}	Top-drive effective rotary inertia	500 kg m^2
M_{bit}	Drill-bit effective mass	5 000 kg
J_{bit}	Drill-bit effective rotary inertia	394 kg m^2

4. Numerical Results

In this section, the drill-string finite element model combined with the standard rotary speed controller is first applied to the analysis of a typical drilling condition to show how the drill-string torsional vibrations and stick-slip frictional resisting torque at the drill-bit may affect the drilling performance. Then, some numerical experiments are performed to evaluate the effect of top-drive axial excitations on the drilling performance.

The typical drilling parameters presented by Tucker and Wang (2003) are considered here and are shown in Table 1. Using these parameters, a typical drilling condition is simulated, for which the target angular velocity is 100 RPM (10.47 rad/s) and the target weight-on-bit is 120 kN. From these settings and using Eq.(4), the target rate-of-penetration is 17.3 m/h. The feedback control parameters are set to $k_p = 200$ and $k_i = 100$ and the drill-string is assumed to have an initial uniform angular velocity of 70 RPM (7.33 rad/s).

The drill-string was divided in 7 finite elements, leading to a total of 15 nodal degrees-of-freedom (the drill-bit axial displacement is locked to its static value). The control and frictional torques, at top-drive and drill-bit respectively, are evaluated as functions of the state variables, whereas the axial excitation force is evaluated as a function of both state variables and time. The resulting equations of motion were rewritten in the state space and implemented in MATLAB. The equations of motion are then numerically integrated for a 100 seconds time interval using a stiff ODE integrator of MATLAB (ode15s: a quasi-constant step size implementation in terms of backward differences of the Klopfenstein-Shampine family of Numerical Differentiation Formulas of orders 1-5).

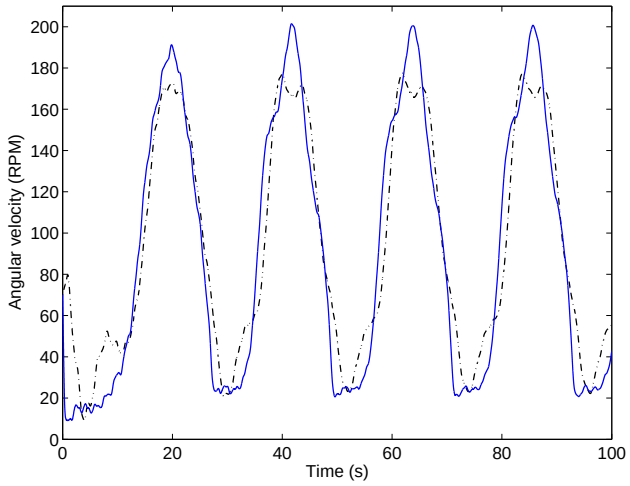

Figure 4. Angular velocities at top-drive (dash-dotted) and drill-bit (solid) for constant WOB and standard PI rotary speed control.

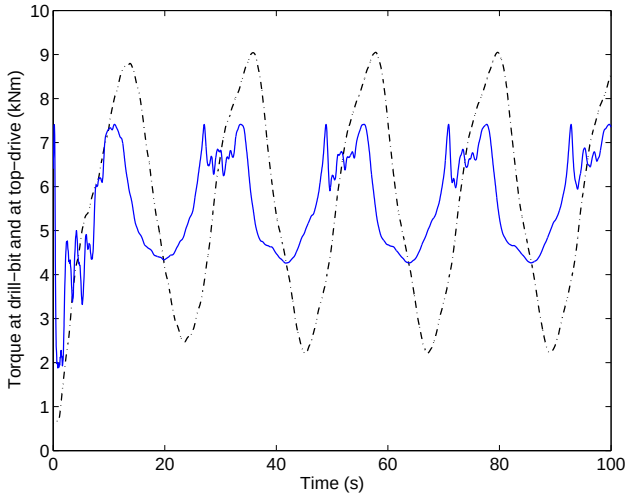

Figure 5. Control torque (dash-dotted) and frictional torque (solid) for constant WOB and standard PI rotary speed control.

Figure 4 shows the angular velocities at the top-drive and drill-bit. It can be observed that both angular velocities exhibit oscillatory motion around the target angular velocity of 100 RPM, although the driving torque is meant to maintain the top-drive angular velocity at 100 RPM. This oscillatory behavior is mainly due to the stick-slip at the drill-bit/formation interface and has a period of around 21.9 s (that is, a frequency of around 0.287 rad/s). More importantly, the peak angular velocity is about double the target one while the minimum angular velocity is only 20% the target one. The angular

velocity oscillatory behavior may lead to smaller rate-of-penetration and even drill-bit failure.

The control driving torque at the top-drive and the frictional resisting torque at the drill-bit are shown in Figure 5. The figure shows that the control driving torque exhibits also an oscillatory behavior. This is often observed as a signature for stick-slip condition (Tucker and Wang, 2003). The frictional torque also presents an oscillatory behavior but it is limited to 7.4 kN.m, which is the maximum torque allowed by the model for a 120 kN weight-on-bit (see also Figure 3). In fact, it can be readily seen in Figures 4 and 5 that the maximum frictional torque is achieved for the smaller values of drill-bit angular velocity.

Due to the oscillatory behavior of drill-bit angular velocity, the rate-of-penetration is also oscillatory presenting start-stop type progression, as shown in Figure 6. This can lead to slower penetration, that is smaller drilling performance. The results presented here matches very well the simulation results presented by Tucker and Wang (2003).

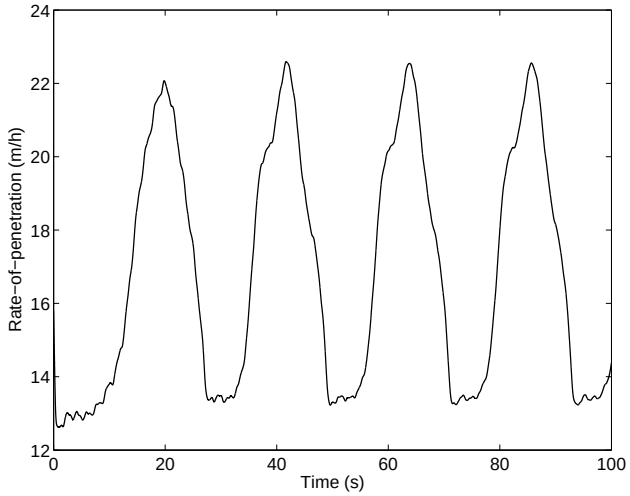

Figure 6. Rate-of-penetration for constant WOB and standard PI rotary speed control.

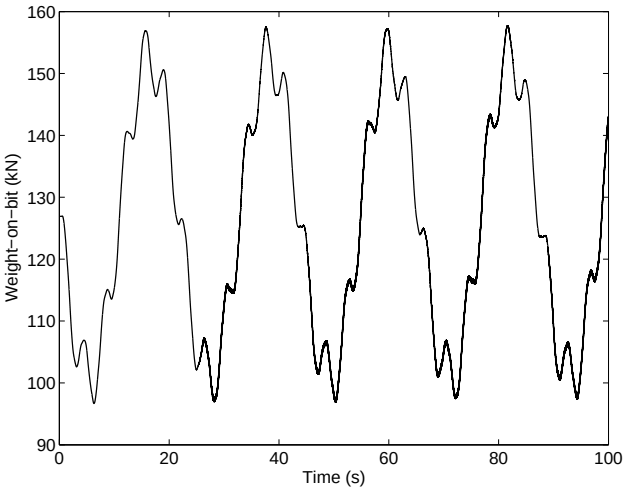

Figure 7. Varying weight-on-bit due to axial excitation at top-drive.

With the objective of alleviating the rate-of-penetration oscillations, an alternative drilling condition is considered, for which a varying weight-on-bit is assumed. In fact, since the rate-of-penetration is a function of angular velocity and weight-on-bit, it is possible to evaluate a time-varying weight-on-bit in order to minimize variations on the rate-of-penetration. This is done here using a sinusoidal axial excitation at the top-drive with amplitude 25 kN (21% of the static weight-on-bit) and frequency 0.287 rad/s (the observed frequency for the angular velocity oscillation in the constant weight-on-bit case). The resulting weight-on-bit was evaluated through simulation and is shown in Figure 7. Notice that the resulting weight-on-bit is not purely sinusoidal, since there are frequency components corresponding to axial vibrations that are excited in the drill-string.

Figure 8 shows the angular velocities at the top-drive and drill-bit for the varying weight-on-bit drilling condition. Notice that the angular velocity behavior follows that of the weight-on-bit. In particular, the first peak of the angular velocity was displaced from around 20 s to around 25 s, so that the angular velocity reaches its peaks at the same time the weight-on-bit reaches its valleys. It can also be observed that the angular velocity oscillation amplitude has increased, with the peak angular velocity reaching 2.2 times the target one and the minimum angular velocity decreasing to only 15% of the target one.

The rate-of-penetration for the case of variable weight-on-bit is shown in Figure 9. It can be observed that, although both angular velocity and weight-on-bit exhibit oscillatory behavior, proper setting of weight-on-bit frequency and amplitude may significantly reduce the oscillation amplitude of the rate-of-penetration. Moreover, the remaining oscillatory behavior is mostly due to axial vibrations induced by the top-drive axial excitation.

It is also worthwhile to include a direct velocity feedback controller into the axial excitation so as to minimize the remaining oscillatory behavior due to the propagation of axial waves. Hence, the axial force at the top-drive is written as

$$F_{\rm top} = F_{\rm top}^{\rm st} + F_{\rm top}^{\rm ex} + F_{\rm top}^{\rm fb} \tag{8}$$

where $F_{\rm top}^{\rm st}$ is the static weight-on-hook (WOH), with magnitude equal to the system weight minus the WOB, $F_{\rm top}^{\rm ex} = 25\sin(.287\ t)\text{kN}$ is the sinusoidal axial excitation, and $F_{\rm top}^{\rm fb}$ is the direct velocity feedback written as

$$F_{\rm top}^{\rm fb} = -k_d \dot{u}_0 \tag{9}$$

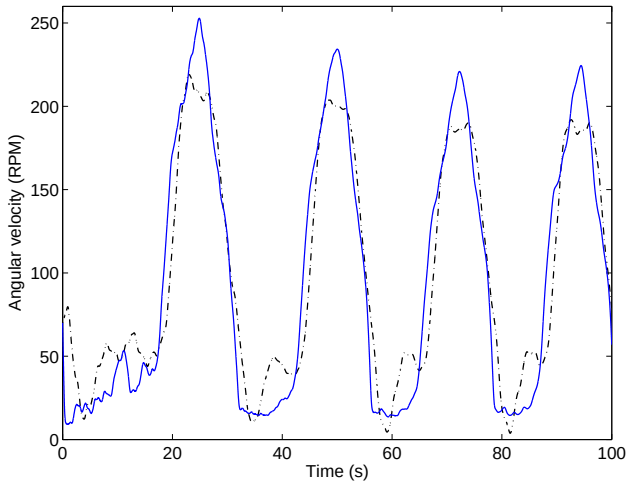

Figure 8. Angular velocities at top-drive (dash-dotted) and drill-bit (solid) for varying WOB and standard PI rotary speed control.

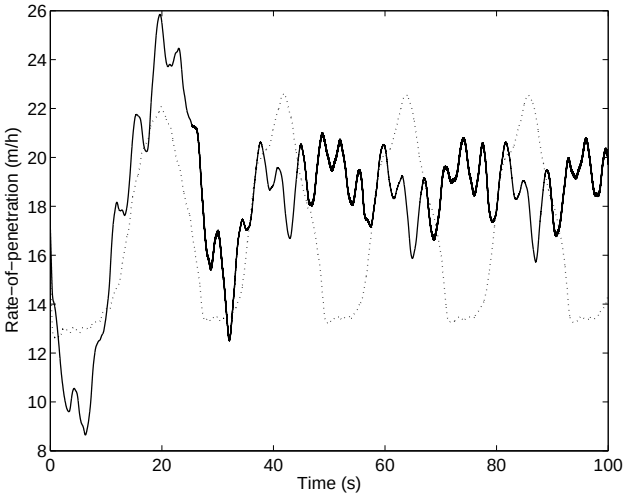

Figure 9. Rate-of-penetration for constant (dotted) and varying (solid) WOB and standard PI rotary speed control.

Figure 10 shows the varying weight-on-bit due to axial excitation at top-drive combined with the derivative axial feedback for a control gain $k_d = 10^4$. It can be observed that the feedback controller eliminates the higher-frequency axial vibrations observed in Figure 7 (repeated in Figure 10 for comparison purposes), yielding a sinusoidal oscillation on the WOB. The effect of the controlled axial excitation on the ROP can be observed in Figure 11. It shows the rate-of-penetration for standard PI rotary speed control combined to constant and varying WOB, without and with axial derivative feedback. Notice that higher-frequency oscillations in the rate-of-penetration are eliminated by the feedback controller and, thus, leading to a smoother penetration. It can be also be seen in Figure 11 however that the ROP still oscillates due to higher-frequencies components of the angular velocities, which are not affected by the axial feedback.

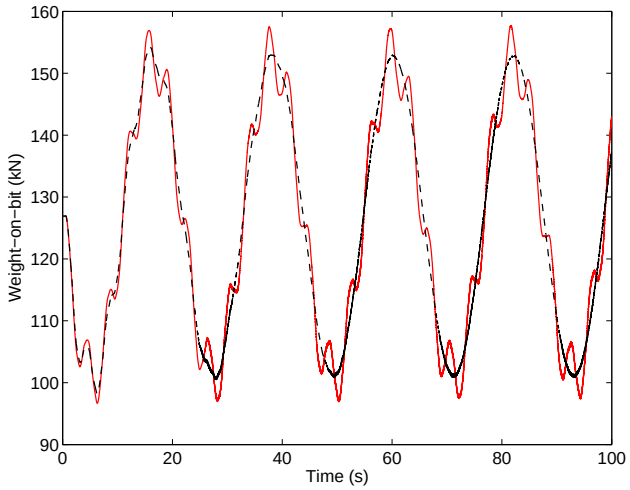

Figure 10. Varying weight-on-bit due to axial excitation at top-drive without (solid) and with (dashed) derivative axial feedback.

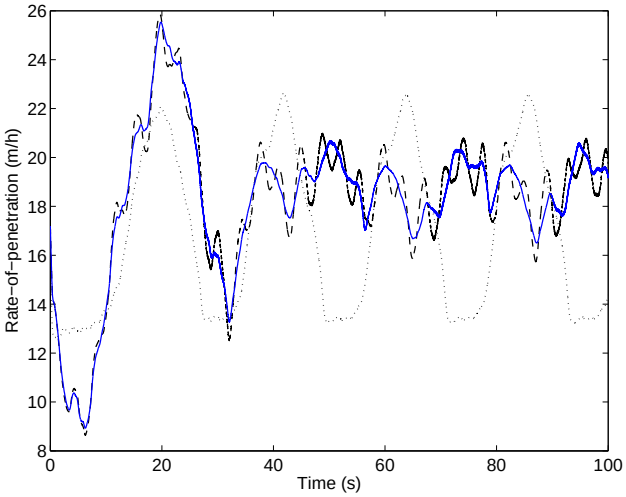

Figure 11. Rate-of-penetration for standard PI rotary speed control combined to constant (dotted) and varying WOB, without (dashed) and with (solid) axial derivative feedback.

Notice that the axial excitation not only diminishes the oscillation amplitude of the ROP but may also increase the average ROP, and thus penetration. Indeed, the average ROP for a constant WOB was found to be 16.83 m/h, yielding a total penetration of 0.468 m after 100 s, whereas the average ROP and total penetration for a varying WOB, both with and without axial derivative feedback, were found to be 18.24 m/h and 0.507 m. Figure 12 shows the accumulated penetration for the standard PI rotary speed control combined to constant and varying WOB, without and with axial derivative feedback. Notice that the axial derivative feedback does not improve the penetration rate, when compared to uncontrolled axial excitation, but it does make the penetration smoother.

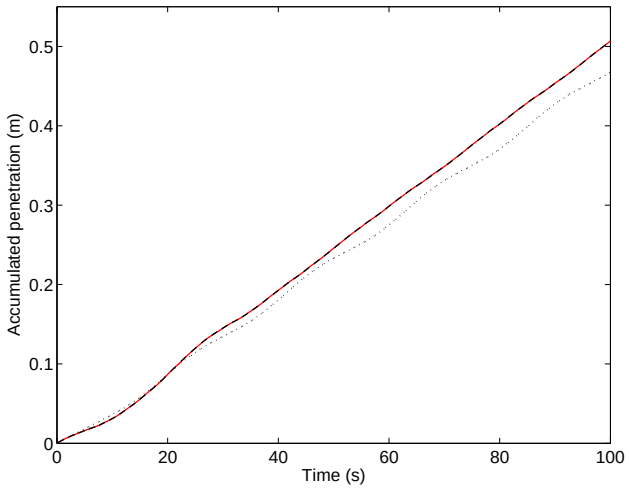

Figure 12. Accumulated penetration for standard PI rotary speed control combined to constant (dotted) and varying WOB, without (solid) and with (dashed) axial derivative feedback.

5. Conclusions

A finite element model for axial-torsional coupled vibrations of drill-strings was presented and used to evaluate the effect of stick-slip phenomenon on a drill-string rotary speed control. The drill-bit-formation interaction was modelled using a nonlinear regularized friction model which accounts for the dynamical behavior of the reaction force at bit-formation interface. Oscillatory behavior of angular velocity and, consequently, of drilling rate-of-penetration, due to a standard PI control driving system applied to a highly nonlinear problem, was observed, in accordance to previous published results. An alternative drilling condition using axial excitations at the top-drive to minimize rate-of-penetration oscillations was tested. It was shown that, although both angular velocity and weight-on-bit exhibit oscillatory behavior, proper setting of axial excitation frequency and amplitude may significantly reduce the oscillation amplitude of the rate-of-penetration. Then, a direct velocity feedback controller was included into the axial excitation system to minimize the higher-frequencies axial vibrations and yield a purely sinusoidal weight-on-bit. Consequently, it was shown that higher-frequency oscillations in the rate-of-penetration are eliminated, thus, leading to a smoother penetration. Other control strategies for both rotary speed control and rate-of-penetration maximization will be considered in the future.

6. References

Christoforou, A.P. and Yigit, A.S., 2003, "Fully coupled vibrations of actively controlled drillstrings", *Journal of Sound and Vibration* **267**:1029–1045.

Jansen, J.D. and van den Steen, L., 1995, "Active damping of self-excited torsional vibrations in oil well drillstrings", *Journal of Sound and Vibration* **179**:647–668.

Plácido, J.C.R., Santos, H.M.R. and Galeano, Y.D., 2004, "Drillstring vibration and wellbore instability", *Journal of Energy Ressources Technology* **124**:217–222.

Trindade, M.A. and Sampaio, R., 2002, "Dynamics of beams undergoing large rotations accounting for arbitrary axial deformation", *Journal of Guidance, Control, and Dynamics* **25**(4):634–643.

Trindade, M.A., Wolter, C. and Sampaio, R., 2005, "Karhunen-Loève decomposition of coupled axial/bending vibrations of beams subject to impacts", *Journal Sound and Vibration* **279**(3-5):1015–1036.

Tucker, R.W. and Wang, C., 2003, "Torsional vibration control and cosserat dynamics of a drill-rig assembly", *Meccanica* **38**:143–159.

Yigit, A.S. and Christoforou, A.P., 2000, "Coupled torsional and bending vibrations of actively controlled drillstrings", *Journal of Sound and Vibration* **234**:67–83.

7. Responsibility notice

The authors are the only responsible for the printed material included in this paper.